European Review for Medical and Pharmacological Sciences 2022; 26: 3800-3806

LncRNA H19 inhibits proliferation and enhances apoptosis of nephroblastoma cells by regulating the miR-675/TGFBI axis

H.-C. LIU[1], W.-Y. ZHU[2], L.-Y. REN[2]

[1]Department of Neonatal Care Unit, Shandong Province Shanxian Central Hospital, Heze, China
[2]Department of Pediatrics, Shandong Province Shanxian Central Hospital, Heze, China

Abstract. – OBJECTIVE: To investigate the influences of long non-coding ribonucleic acid (lncRNA) H19 on proliferation and apoptosis of nephroblastoma cells.

MATERIALS AND METHODS: A total of 5 pairs of nephroblastoma tissues and paraneoplastic tissues were obtained. Gene expression levels of lncRNA H19, microRNA (miR)-675, and transforming growth factor beta induced (TGFBI) were detected *via* quantitative Reverse Transcription-Polymerase Chain Reaction (qRT-PCR). Their regulatory effects on the viability of nephroblastoma cells were examined by Cell Counting Kit-8 (CCK-8) assay. Finally, the apoptosis level in each group was detected through TUNEL assay, and the protein expressions of TGFBI and Caspase-8 were examined using Western blotting (WB) assay.

RESULTS: The gene expression levels of lncRNA H19 and miR-675 were markedly downregulated in nephroblastoma tissues ($p<0.05$), while that of TGFBI was notably upregulated ($p<0.05$). LncRNA H19 could reduce the proliferative ability of HFWT cells ($p<0.05$) and stimulates apoptosis rate ($p<0.05$). It upregulated the expressions of miR-675 and Caspase-8 ($p<0.05$), and downregulated TGFBI ($p<0.05$). Besides, miR-675 was able to upregulate Caspase-8 ($p<0.05$) and downregulate TGFBI ($p<0.05$). In addition, the protein expression of Caspase-8 was downregulated ($p<0.05$), while that of TGFBI was upregulated ($p<0.05$) after the knockdown of miR-675 in HFWT cells.

CONCLUSIONS: LncRNA H19 may inhibit TGFBI expression by regulating miR-675 level, so as to weaken the proliferation and enhance the apoptosis of nephroblastoma cells.

Key Words:
Nephroblastoma, LncRNA H19, MiR-675, TGFBI, Proliferation, Apoptosis.

Introduction

Nephroblastoma, also known as Wilms tumor, is not only the second most common extracranial solid tumor in children but also the most common malignant renal tumor, accounting for over 95% of all kidney tumors in children[1]. The overall survival rate of the patients with nephroblastoma has been raised to over 90% with the improvement on surgery, radiotherapy, and chemotherapy[2].

Transcription changes of long non-coding ribonucleic acid (lncRNAs) in cancer transcriptome is one of the most ubiquitous phenomena[3]. A great number of studies[4-7] have revealed that lncRNAs play important roles in tumorigenesis. Similar to protein-coding genes, lncRNAs are abnormally expressed during the occurrence and development of cancers, which is manifested in the changes of gene copy numbers and promoter deoxyribonucleic acid (DNA) methylation[8,9].

Coorens et al[9] reported in the latest study that clonal amplification is exacerbated in 14 out of 23 (61%) cases of renal tissues with normal morphology before the development of nephroblastoma. The clonal amplification is triggered by the mutation of somatic cells that are existent in both tumor tissues and normal tissues but absent in blood cells. They also discovered that the hypermethylation of H19 locus occurs in 58% of amplification, and the H19 locus is a known driving force of nephroblastoma progression[9]. Although some functions of H19 in cancers have been identified, the specific regulatory mechanism remains unclear. In this research, therefore, the influences of lncRNA H19 on the proliferation and apoptosis of nephroblastoma cells were investigated, so as to clarify the pathogenic mechanism of lncRNA H19 in tumor development.

Materials and Methods

Main Materials

Human nephroblastoma HFWT cell American Type Culture Collection (ATCC; Manassas, VA,

Corresponding Author: Liying Ren, MM; e-mail: renliyingrenliying@163.com

Table I. Primer sequences for lncRNA H19, miR-675, TGFBI, and GAPDH detection

Name	Sequence
H19 F	5'-CAGCTGCCACGTCCTGTAA-3'
H19 R	5'-GCGCCTACTCCACACTCCTC-3'
MiR-675 F	5'-TGGTGCGGAGAGGGC-3'
MiR-675 R	5'-GAACATGTCTGCGTATCTC-3'
TGFBI F	5'-TGCTCCCACAAATGAAGCCT-3'
TGFBI R	5'-GCCTCCGCTAACCAGGATTT-3'
GAPDH F	5'-GTCAAGGCTGAGAACGGGAA-3'
GAPDH R	5'-AAATGAGCCCCAGCCTTCTC-3'

USA), SYBR Green reverse transcription (RT) Master Mix kit (TaKaRa, Otsu, Shiga, Japan), Dulbecco's Modifed Eagle's Medium (DMEM; Hyclone, South Logan, UT, USA) medium, fetal bovine serum (FBS; Gibco, Rockville, MD, USA), L-glutamine, nonessential amino acids, 2.5% trypsin + 0.02% ethylene diamine tetraacetic acid (EDTA) and phosphate-buffered saline (PBS; Gibco, Rockville, MD, USA), pGreenPuro™ short hairpin RNA (shRNA) vector (System Biosciences, Beijing, China), Lipofectamine 2000 and TRIzol (Invitrogen, Carlsbad, CA, USA), antibodies of ABCG2, TNFR1, Caspase-3, and β-actin (Abcam, Cambridge, MA, USA), miRNA RT kit (Applied Biosystems, Foster City, CA, USA), and 0.45 μm pinhole filter (Millipore, Billerica, MA, USA).

Cell Culture

Human nephroblastoma HFWT cells were cultured in Dulbecco's Modified Eagle's Medium containing 15% FBS in an incubator under 5% CO_2 at 37°C. Cell passage was conducted when the cell confluence was about 90%. Next, the cells were washed once in PBS and digested in 2.5% trypsin + 0.02% EDTA, followed by incubation at 37°C for 2-3 min. The digestion was terminated by adding fresh medium. Cells were passaged at a ratio of 1:3-1:6.

Lentivirus Infection of Cells

The designed oligonucleotide miR-675 or anti-miR-675 was separately cloned into pGreenPuro™ shRNA vector according to Lentivector cloning and expressing methods. Then, H19 complementary DNA (cDNA) was amplified and cloned into pLV-CMVenh-EGFP vector *via* Polymerase Chain Reaction (PCR). 293FT cells seeded in a 10-cm plate were transfected with 2.5 μg of pLV-CMVenh-EGFP vector, pGreenPuro™ shRNA vector or empty vector, respectively. Later, 5 μg of pCMV-dR8 and 5 μg of pMD2G were mixed with Lipofectamine 2000 at 1:3 in 1 mL of Opti-MEM. 48 h later, the medium was filtered using a 0.45 μm filter for subsequent cell infection. Finally, the cells were cultured in an incubator with 5% CO_2 at 37°C, and the abundance of H19 or miR-675 in each group of cells was determined after infection.

Extraction of Total RNA and Quantitative Real Time-Polymerase Chain Reaction (qRT-PCR)

The tissues were ground in liquid nitrogen, lysed in TRIzol, and mixed evenly. After 5-min reaction at room temperature, 200 μL of chloroform was applied and the mixture was centrifuged at 4°C, 12,000 rpm for 10 min. Then, the supernatant was obtained, mixed with an equal volume of isopropyl alcohol and centrifuged at 4°C, 12,000 rpm for 15 min. Later, the precipitant was washed in 75% ethanol twice and dissolved in an appropriate amount of diethyl pyrocarbonate (DEPC)-treated water (Beyotime, Shanghai, China). The RNA concentration was detected using a NanoDrop spectrophotometer. Next, the primers were designed by Premier 6.0 software and synthesized by Sangon Biotechnology (Shanghai, China) Co., Ltd. The primer sequences of H19, miR-675, transforming growth factor beta induced (TGFBI) and glyceraldehyde-3-phosphate dehydrogenase (GAPDH) were shown in Table I. MiR-675 was synthesized into first-strand cDNA using the qScript microRNA cDNA kit, and the total RNA was synthesized into cDNA by the random primers from RT Master Mix kit for H19, TGFBI, and GAPDH. Next, qRT-PCR was performed using the SYBR Green Real-Time PCR Master Mix kit and ABI 7500 sequence detection system (Applied Biosystems, Foster City, CA, USA) in accordance with the manufacturer's protocol. The transcription level was evaluated *via* cycle threshold (Ct) value. The target amount of standardized internal reference was calculated though $2^{-\Delta\Delta Ct}$ method.

Cell Counting Kit-8 (CCK-8) Assay

The cells in good growth status were inoculated into a 96-well plate (5×10^3 cells/well), with 6 replicate wells for each group, followed by cell culture in the incubator with 5% CO_2 at 37°C for 1, 2 or 3 d. After that, the medium was discarded, and fresh medium containing 10 μL of CCK-8 detection solution (Dojindo Molecular Technologies,

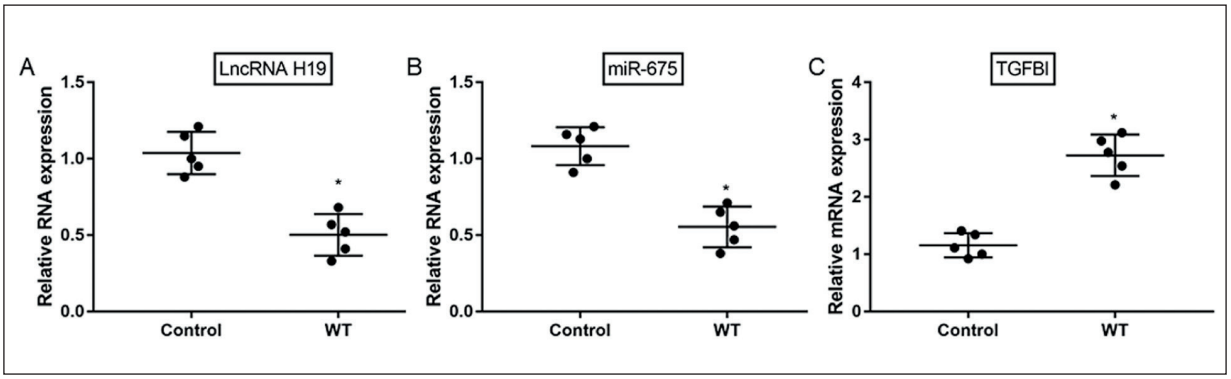

Figure 1. Gene expression levels of lncRNA H19, miR-675 and TGFBI detected *via* qRT-PCR. *$p<0.05$, with significant difference between two groups.

Kumamoto, Japan) was added into each well. Four hours later, the optical density (OD) value at the wavelength of 450 nm was measured using a microplate reader. The experiment was repeated for 3 times, and the average value of the experimental results was taken as the final result.

One-Step Terminal Deoxynucleotidyl Transferase-Mediated dUTP Nick End Labeling (TUNEL) Apoptosis Assay

Differently treated cells were washed with PBS once, fixed in a proper amount of 4% paraformaldehyde for 15 min, washed with PBS for 3 times and permeabilized in an appropriate amount of 0.1% Triton X-100 (Solarbio, Beijing, China) for 2 min. After that, the samples were incubated with 50 μL of TUNEL detection solution at room temperature for 1 h after washing with PBS for 3 times. Then, the samples were washed in PBS for 3 times again and mounted in a suitable amount of anti-fluorescence quencher, followed by observation and photography under a fluorescence microscope.

Western Blotting

The transfected cells were lysed using cell lysis buffer (Qincheng Biotech, Shanghai, China; Cat no: QC25-05099), followed by centrifugation at 13,000 rpm to extract the total protein. Protein concentration was detected through bicinchoninic acid (BCA) method (Pierce, Rockford, IL, USA). Next, the proteins were separated *via* 8% sodium dodecyl sulphate-polyacrylamide gel electrophoresis (SDS-PAGE) and transferred onto polyvinylidene difluoride (PVDF) membranes (Millipore, Billerica, MA, USA). Subsequently, the membrane was sealed in 5% skim milk powder and 0.1% Tris-buffered saline-Tween 20, and incubated with primary antibodies of TFGBI (ab170874; 1:500), Caspase-8 (ab138485; 1:500) and β-actin (ab8227; 1:500) separately by gently shaking at 4°C overnight. After that, secondary goat anti-rabbit (HRP) IgG antibody (ab6721; 1:2000) were added for incubation, and the proteins to be detected were subjected to exposure using enhanced chemiluminescence (ECL) reagent (Thermo Fisher Scientific, Waltham, MA, USA). All the antibodies were all purchased from Abcam (Cambridge, MA, USA).

Statistical Analysis

Statistical Product and Service Solutions (SPSS) 20.0 software (IBM Corp., Armonk, NY, USA) was used for data recording and processing. The data in each group were presented as mean ± standard deviation ($\chi \pm s$). The independent-samples *t*-test was adopted for comparison between groups. $p<0.05$ suggested that the difference was statistically significant.

Results

LncRNA H19 Expression in Nephroblastoma

The nephroblastoma tissues and normal paraneoplastic tissues were collected. Gene expression levels of lncRNA H19, miR-675, and TGFBI were examined *via* qRT-PCR. Lower gene expression levels of lncRNA H19 and miR-675 ($p<0.05$) (Figure 1A and 1B) and an evidently higher gene expression level of TGFBI were observed in nephroblastoma tissues than normal paraneoplastic tissues ($p<0.05$) (Figure 1C).

HFWT Cell Transfection

HFWT cells were subjected to lentivirus transfection. QRT-PCR was applied to verify the trans-

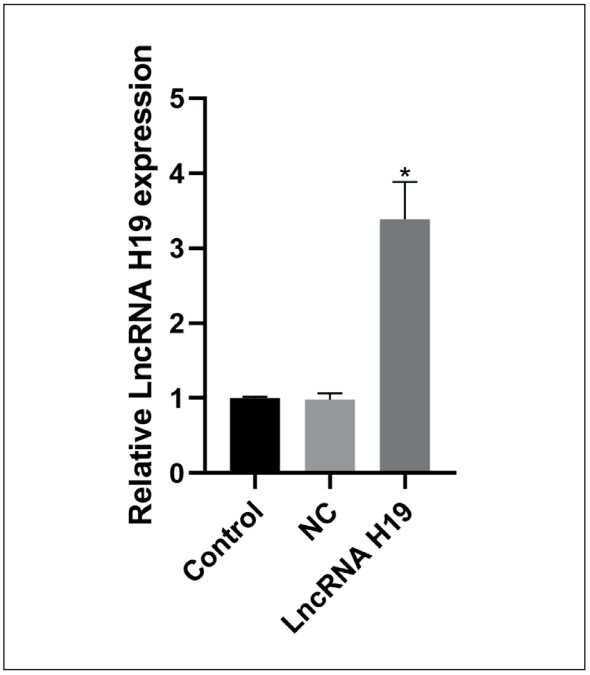

Figure 2. Abundance of lncRNA H19 determined through qRT-PCR after cell transfection. *p<0.05 *vs.* other groups, with significant differences.

fection efficacy and it was confirmed that lncRNA H19 expression was effectively intervened following transfection (p<0.05) (Figure 2).

Influence of LncRNA H19 on Cell Proliferation

According to the CCK-8 assay results of cell proliferation, the cells transfected with lncRNA H19 had significantly reduced proliferative ability compared with those of the controls (p<0.05) (Figure 3).

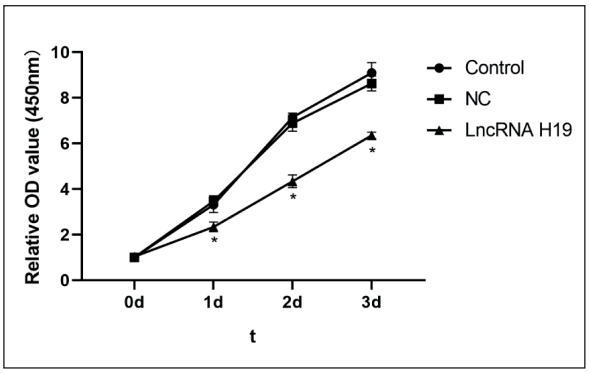

Figure 3. Proliferative ability of cells detected *via* CCK-8 assay. *p<0.05 *vs.* other groups, with significant differences.

Influence of LncRNA H19 on Cell Apoptosis

It was manifested in one-step fluorescence TUNEL assay that the apoptosis of HFWT cells transfected with lncRNA H19 was enhanced distinctly (p<0.05) (Figure 4).

Relationship Between LncRNA H19 and MiR-675

In order to further verify the regulatory relationship between lncRNA H19 and miR-675, qRT-PCR was applied to measure their RNA expressions. It was displayed that the expression level of miR-675 remarkably rose in HFWT cells transfected with lncRNA H19 (p<0.05), which was notably downregulated after miR-675 expression was repressed (p<0.05) (Figure 5A). Based on the CCK-8 assay results of cell proliferation, the knockdown of miR-675 markedly increased the proliferative ability of the cells (p<0.05) (Figure 5B).

Correlations of LncRNA H19 and miR-675 with Expressions of TGFBI and Apoptosis-Related Proteins

Western blotting assay revealed that both lncRNA H19 and miR-675 significantly downregulated the protein expression level of TGFBI (p<0.05) and prominently upregulated the protein expression level of Caspase-8 (p<0.05). Besides, the protein expression level of TGFBI markedly increased (p<0.05), while that of Caspase-8 evidently decreased (p<0.05) by knockdown of miR-675 (Figure 6).

Discussion

H19, a non-coding RNA, is highly expressed in the endoderm and mesoderm of embryo, but its expression is suppressed in a majority of tissues after birth[10-12]. Hao et al[13] demonstrated that H19 possesses the tumor-suppressor activity. H19 induces growth inhibition and morphological changes in RD and nephroblastoma cells. In addition, colony formation and tumorigenesis are also influenced by H19 in nude mice. According to the latest study conducted by Coorens et al[9], hypermethylation of H19 locus is observed in 58% of amplified nephroblastoma cells, suggesting that H19 locus is a known driving force of nephroblastoma progression. Zhu et al[14] found that the upregulated H19 in metastatic prostate cancer cells P69 and PC3 remarkably increases

the level of miR-675 and inhibits cell migration. Similar results were obtained by analyzing the nephroblastoma tissues in this research. Specifically, the expression level of H19 in tumor tissues was notably lower than that in normal paraneoplastic tissues. So far, there are also several previous publications which reported the role of H19 in nephroblastoma. Li et al[15] described the complexity of H19 function and the dual role of H19 polymorphisms in the development of nephroblastoma. However, the specific role and potential molecular mechanism of H19 in the tumorigenesis of nephroblastoma still remains to be further explored.

In the present study, we found that H19 markedly influenced proliferation and apoptosis of nephroblastoma cells, implying the involvement of H19 in the development of nephroblastoma. Meanwhile, H19 stimulates the production and maturation of miR-675 precursor in addition to its own functions. MiR-675 facilitates the proliferation of colon cancer cells[16]. Serving as a developmental reservoir of miR-675, H19 inhibits growth and Igf1r, illustrating that H19 and miR-675 have complicated effects under varying physiological and pathological conditions[17]. Our findings uncovered that H19 and miR-675 were downregulated in nephroblastoma tissues. Moreover, the expression of miR-675 in cells was upregulated after overexpression of H19.

The gene mutation or protein loss of TGFBI, a TGF-β1-induced secretory protein, is closely associated with the cell proliferation, tumor progression, and angiogenesis[18,19]. TGFBI product is a component of proteolytic enzyme degradation in extracellular matrix, which mediates cell adhesion and migration by the interaction of integrin receptors a3h1, avh3, and avh5 with integrins[20,21]. TGFBI enhances the integrin-dependent cell adhesion and motility[22]. The tumorigenesis in esophageal cancer, oral squamous cell carcinoma and glioma are also regulated by TGFBI[23,24]. Ma et al[25] illustrated that TGFBI strengthens the metastatic property of colon cancer *in vivo*. In particular,

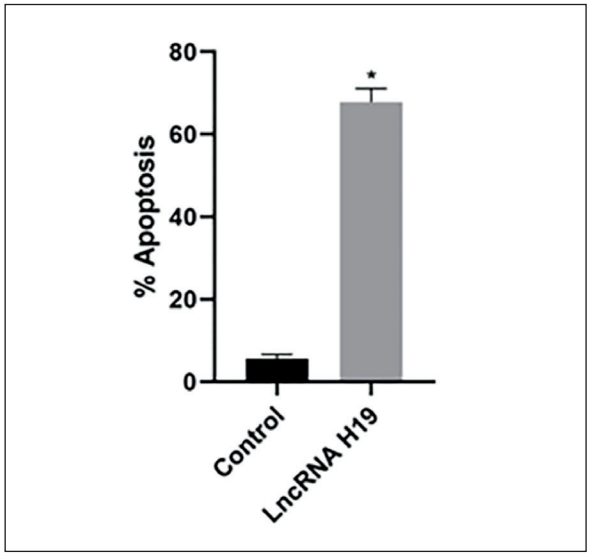

Figure 4. TUNNEL assay showed that lncRNA H19 distinctly enhances the cell apoptosis ($p<0.05$).

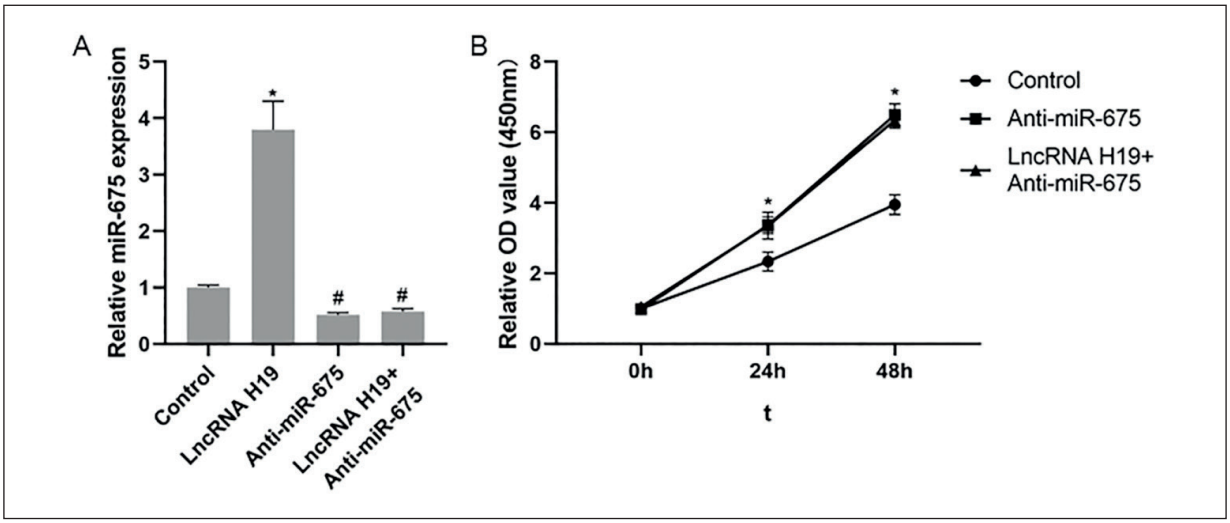

Figure 5. Relationship between lncRNA H19 and miR-675 and their influences on cell proliferation. **A,** Expression level of miR-675 determined by qRT-PCR. **B,** Influences of lncRNA H19 and miR-675 on cell proliferation. *&#$p<0.05$ *vs.* other groups, with significant differences.

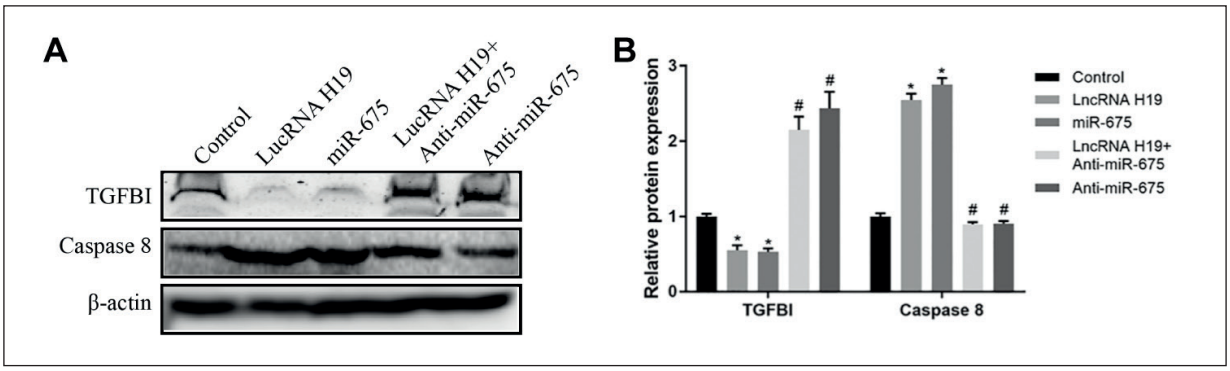

Figure 6. Correlations of lncRNA H19 and miR-675 with TGFBI expression. ***A,*** Diagram of WB assay. ***B,*** Relative protein expressions. *&#*p*<0.05 *vs.* other groups, with significant differences.

TGFBI increases cell extravasation depending on the integrin-Src signaling pathway. In addition, TGFBI promotes the migration and invasion of renal cell carcinoma[26], indicating that TGFBI has a close correlation with cancer metastasis. Zhu et al[14] demonstrated that TGFBI is the target of miR-675, and the expression levels of H19 or miR-675 in P69 cells are negatively correlated with TGFBI expression. Dual-Luciferase reporter gene assay revealed that miR-675 represses the translation of TGFBI by directly binding to the 3'-UTR of its mRNA, illustrating that the H19/miR-675 axis may have potentials in diagnosing and treating advanced prostate cancer[14]. In this research, there was a negative regulatory relationship between miR-675 and TGFBI expressions, and H19 expression also negatively regulated TGFBI expression, which are consistent with the findings on the prostate cancer[14]. Besides, it was discovered through the analysis on relative levels of apoptosis-related proteins that the H19/miR-675 axis could facilitate the cell apoptosis in nephroblastoma.

Conclusions

In summary, the present study demonstrated that lncRNA H19 may inhibit TGFBI expression by regulating miR-675 level, thus attenuating the proliferation and enhancing the apoptosis of nephroblastoma cells. Our findings may provide new target for the diagnosis and therapeutics of nephroblastoma.

Conflict of Interest

The authors declare that they have no conflict of interest.

References

1) Milford K, DeCotiis K, Lorenzo A. Wilms tumor: a review of current surgical controversies. Transl Androl Urol 2020; 9: 2382-2392.
2) Irtan S, Ehrlich PF, Pritchard-Jones K. Wilms tumor: "state-of-the-art" update, 2016. Semin Pediatr Surg 2016; 25: 250-256.
3) Iyer MK, Niknafs YS, Malik R, Singhal U, Sahu A, Hosono Y, Barrette TR, Prensner JR, Evans JR, Zhao S, Poliakov A, Cao X, Dhanasekaran SM, Wu YM, Robinson DR, Beer DG, Feng FY, Iyer HK, Chinnaiyan AM. The landscape of long noncoding RNAs in the human transcriptome. Nat Genet 2015; 47: 199-208.
4) Yang L, Zheng S, Ge D, Xia M, Li H, Tang J. LncRNA-COX2 inhibits Fibroblast Activation and Epidural Fibrosis by Targeting EGR1. Int J Biol Sci 2022; 18: 1347-1362.
5) Prensner JR, Chinnaiyan AM. The emergence of lncRNAs in cancer biology. Cancer Discov 2011; 1: 391-407.
6) Zheng S, Wan L, Ge D, Jiang F, Qian Z, Tang J, Yang J, Yao Y, Yan J, Zhao L, Li H, Yang L. LINC00266-1/miR-548c-3p/SMAD2 feedback loop stimulates the development of osteosarcoma. Cell Death Dis 2020; 11: 576.
7) Zhu S, Li W, Liu J, Chen CH, Liao Q, Xu P, Xu H, Xiao T, Cao Z, Peng J, Yuan P, Brown M, Liu XS, Wei W. Genome-scale deletion screening of human long non-coding RNAs using a paired-guide RNA CRISPR-Cas9 library. Nat Biotechnol 2016; 34: 1279-1286.
8) Wang Z, Yang B, Zhang M, Guo W, Wu Z, Wang Y, Jia L, Li S, Xie W, Yang D. LncRNA epigenetic landscape analysis identifies EPIC1 as an oncogenic lncRNA that interacts with MYC and promotes cell-cycle progression in cancer. Cancer Cell 2018; 33: 706-720.
9) Coorens T, Treger TD, Al-Saadi R, Moore L, Tran M, Mitchell TJ, Tugnait S, Thevanesan C, Young MD, Oliver T, Oostveen M, Collord G, Tarpey PS, Cagan A, Hooks Y, Brougham M, Reynolds BC,

Barone G, Anderson J, Jorgensen M, Burke G, Visser J, Nicholson JC, Smeulders N, Mushtaq I, Stewart GD, Campbell PJ, Wedge DC, Martincorena I, Rampling D, Hook L, Warren AY, Coleman N, Chowdhury T, Sebire N, Drost J, Saeb-Parsy K, Stratton MR, Straathof K, Pritchard-Jones K, Behjati S. Embryonal precursors of Wilms tumor. Science 2019; 366: 1247-1251.

10) Lustig O, Ariel I, Ilan J, Lev-Lehman E, De-Groot N, Hochberg A. Expression of the imprinted gene H19 in the human fetus. Mol Reprod Dev 1994; 38: 239-246.
11) Wang Y, Wang L, Sui M. Long non-coding RNA H19 promotes proliferation of Hodgkin's lymphoma via AKT pathway. J BUON 2019; 24: 763-769.
12) He H, Wang N, Yi X, Tang C, Wang D. Long non-coding RNA H19 regulates E2F1 expression by competitively sponging endogenous miR-29a-3p in clear cell renal cell carcinoma. Cell Biosci 2017; 7: 65.
13) Hao Y, Crenshaw T, Moulton T, Newcomb E, Tycko B. Tumour-suppressor activity of H19 RNA. Nature 1993; 365: 764-767.
14) Zhu M, Chen Q, Liu X, Sun Q, Zhao X, Deng R, Wang Y, Huang J, Xu M, Yan J, Yu J. LncRNA H19/miR-675 axis represses prostate cancer metastasis by targeting TGFBI. FEBS J 2014; 281: 3766-3775.
15) Li W, Hua RX, Wang M, Zhang D, Zhu J, Zhang S, Yang Y, Cheng J, Zhou H, Zhang J, He J. H19 gene polymorphisms and Wilms tumor risk in Chinese children: a four-center case-control study. Mol Genet Genomic Med 2021; 9: e1584.
16) Tsang WP, Ng EK, Ng SS, Jin H, Yu J, Sung JJ, Kwok TT. Oncofetal H19-derived miR-675 regulates tumor suppressor RB in human colorectal cancer. Carcinogenesis 2010; 31: 350-358.
17) Keniry A, Oxley D, Monnier P, Kyba M, Dandolo L, Smits G, Reik W. The H19 lincRNA is a developmental reservoir of miR-675 that suppresses growth and Igf1r. Nat Cell Biol 2012; 14: 659-665.
18) Thapa N, Lee BH, Kim IS. TGFBIp/betaig-h3 protein: a versatile matrix molecule induced by TGF-beta. Int J Biochem Cell Biol 2007; 39: 2183-2194.
19) Ahmed AA, Mills AD, Ibrahim AE, Temple J, Blenkiron C, Vias M, Massie CE, Iyer NG, McGeoch A, Crawford R, Nicke B, Downward J, Swanton C, Bell SD, Earl HM, Laskey RA, Caldas C, Brenton JD. The extracellular matrix protein TGFBI induces microtubule stabilization and sensitizes ovarian cancers to paclitaxel. Cancer Cell 2007; 12: 514-527.
20) Nam JO, Kim JE, Jeong HW, Lee SJ, Lee BH, Choi JY, Park RW, Park JY, Kim IS. Identification of the alphavbeta3 integrin-interacting motif of betaig-h3 and its anti-angiogenic effect. J Biol Chem 2003; 278: 25902-25909.
21) Jeong HW, Kim IS. TGF-beta1 enhances betaig-h3-mediated keratinocyte cell migration through the alpha3beta1 integrin and PI3K. J Cell Biochem 2004; 92: 770-780.
22) Lee JM, Dedhar S, Kalluri R, Thompson EW. The epithelial-mesenchymal transition: new insights in signaling, development, and disease. J Cell Biol 2006; 172: 973-981.
23) Tomioka H, Morita K, Hasegawa S, Omura K. Gene expression analysis by cDNA microarray in oral squamous cell carcinoma. J Oral Pathol Med 2006; 35: 206-211.
24) Lin B, Madan A, Yoon JG, Fang X, Yan X, Kim TK, Hwang D, Hood L, Foltz G. Massively parallel signature sequencing and bioinformatics analysis identifies up-regulation of TGFBI and SOX4 in human glioblastoma. PLoS One 2010; 5: e10210.
25) Ma C, Rong Y, Radiloff DR, Datto MB, Centeno B, Bao S, Cheng AW, Lin F, Jiang S, Yeatman TJ, Wang XF. Extracellular matrix protein betaig-h3/TGFBI promotes metastasis of colon cancer by enhancing cell extravasation. Genes Dev 2008; 22: 308-321.
26) Shang D, Liu Y, Yang P, Chen Y, Tian Y. TGFBI-promoted adhesion, migration and invasion of human renal cell carcinoma depends on inactivation of von Hippel-Lindau tumor suppressor. Urology 2012; 79: 961-966.